J Fluoresc (2007) 17:418–426
DOI 10.1007/s10895-007-0184-2

Co-luminescence Effect of Heterometallic Terbium–Gadolinium Hybrid Molecular Materials Constructed by Covalent Grafting

Fang-fang Wang · Bing Yan

Received: 18 January 2007 / Accepted: 19 March 2007 / Published online: 18 April 2007

Abstract In this paper, 2-chlorobenzoic acid (CBA) and 2-chloronicotinic acid (CNA) were modified by 3-aminopropyl-trimethoxysilane (APMS) to afford corresponding organic–inorganic monomers (CBA–APMS and CNA–APMS) with two components equipped with covalent bonds which not only can coordinate to RE ions (Tb^{3+} and Gd^{3+}) but also act as a sol–gel precursor. Luminescent hybrid materials consisting of terbium-gadolinium complex covalently bonded to silica-based network have been obtained in situ via a sol–gel approach. Through co-hydrolysis and polycondensation, Tb^{3+} and Gd^{3+} can be introduced in the same organic-inorganic hybrid monomer and then formed Si–O backbones. The co-luminescence effect can be found by studying the luminescence spectra of different ratios of Tb^{3+}–Gd^{3+}, which means that the existence of Gd^{3+} can enhance the luminescence intensity, which may be due to the intramolecular energy transfer between Gd^{3+} and Tb^{3+}.

Keywords Hybrid molecular materials · Intramolecular energy transfer · Co-luminescence · Terbium · Gadolinium

F.-f. Wang · B. Yan (✉)
Department of Chemistry, Tongji University,
Siping Road 1239, Shanghai 200092, China
e-mail: byan@tongji.edu.cn

B. Yan
State Key Lab of Rare Earth Materials Chemistry
and Applications, Peking University, Beijing 100871, China

Introducion

Because the organic–inorganic hybrid materials possess of the mutual advantages of both organic and inorganic networks, they are applied widely in many fields [1, 2]. So, much research on them has been unfolded roundly, and along with the development of inorganic–organic hybrid materials, the synthetic method has been reformed over past 10 years. Among all the synthetic methods, the so–gel approach which is based upon co-hydrolysis and polycondensation, possesses of its unique characteristics, i.e., convenience, low temperature and multifunction [3–7]. These characteristics can be further tailored by altering the sol–gel conditions which can control the microstructure of hybrid materials and enhance the degree of combination between the two phases. With respect to the resulting hybrids, lanthanide organic complexes introduced in silica gel have already been found to display superior emission intensities compared with simple metal ions in inorganic hosts. In addition, for the classification of these new materials, Sanchez and Ribot divide hybrid materials into two major classes according to interaction between the different components or phases [8]. For class I hybrid materials , because of the only weak functional interactions (such as hydrogen bonding, van der Waals force or static effect) between organic and inorganic components [9–11], the problems including the uneven distribution of rare earth complexes, the limitation of doped concentration, the quenching effect of luminescent centers and the separation of different phases are difficult to solve. But class II hybrid materials can achieve true interconnection by covalent grafting which connects inorganic and organic components, so in class II, the organic components are covalently

connected to the inorganic network, they play a role of network modifier. And so far, a few studies concerning covalent grafting hybrid materials have been done and the molecular hybrid materials present monophasic appearance, even if the doped concentration of rare earth complexes is high [12–19].

Inorganic matrices doped with metal complexes especially lanthanide complexes have already been found to show excellent emission intensity owing to the electronic transitions between the 4f energy levels. But up to now, fewer studies have been unfolded on the co-luminescence effect of co-doped rare earth hybrid molecular material and they focus their interest on single rare earth hybrids [20–24]. When Gd^{3+}, La^{3+}, Lu^{3+} and Y^{3+}, respectively, incorporated with Eu^{3+} and then the mixtures were added in the sol–gel matrices, a luminescence enhancement phenomenon was found [25]. A mass of research has been carried out since research worker found that all of the enhancing ions have a stable electronic configuration, such as La^{3+}, Y^{3+}, Gd^{3+} and Lu^{3+}, the 4f shells of which were empty, half-filled and full, respectively [26, 27]. Previous research has concentrated on the RE complex in which luminescence enhancement belongs to intermolecular energy transfer. But, in fact, this sort of complex is hard to prepare, because the effect of luminescence enhancement due to intermolecular energy transfer has not reached people's expectation.

While for molecular hybrid materials systems, the cohydrolysis and copolycondensation process of sol–gel technology make it possible to introduce active rare earth ions and inert rare earth ions into one system readily through covalently bonded Si–O network. In this paper, we reported the synthesis of a series of molecular hybrid materials in which two kinds of RE ions (Tb^{3+} and Gd^{3+}) coordinated to the sol–gel matrix with different ratios and the hybrids showed excellent emission intensity. Because Tb^{3+} and Gd^{3+} combined with the silica-based network through the same co-hydrolysis and polycondensation, then they co-exist in the same silica-based network and intramolecular energy transfer occurs. In order to characterize the structure of intermediate, Fourier transform infrared (FT-IR), UV-Visible Spectrophotometer, HNMR were used, the photophysical properties were discussed in detail.

Experimental

Material

2-chlorobenzoic acid (abbreviated as CBA) and 2-chloronicotinic acid (abbreviated as CNA) were supplied by Lancaster Synthesis Ltd. 3-aminopropyl-trimethoxysilane (abbreviated as APMS) was purchased from Shanghai Yao-Hua chemical company. Solvents used were purified by common methods. Other starting reagents were used as received.

Synthesis of monomers

A typical procedure for the preparation of silylated monomer (CBA–APMS and CNA–APMS) was as follows: CBA/CNA was first converted to acyl chloride by refluxing in excess $SOCl_2$ under argon at 70 ºC for 4 h. After isolation, the acyl chloride was directly reacted with APMS (the molar ratio of CBA or CNA/APMS was 1:1) in ethyl ether in the presence of pyridine. The typical procedure was according to the reaction scheme in Fig. 1. The spectra of FT-IR are seen in Fig. 3; the data of ^{1}HNMR are as follows. CBA–APMS ($C_{13}H_{20}O_4NClSi$): ^{1}HNMR (DMSO) *d*(ppm): 8.01 (1H, *t*), 7.86 (1H, *d*), 7.45(1H, *t*), 7.40 (1H, *d*), 7.23 (1H, *d*), 3.92 (2H, *q*), 3.11 (9H, *s*), 1.05 (2H, *q*), 0.21 (2H, *q*). CNA–APMS ($C_{12}H_{19}O_4N_2ClSi$): ^{1}HNMR (DMSO) *d*–(ppm): 8.41 (1H, *d*), 8.24 (1H, *d*), 7.68 (1H, *t*), 7.51 (1H, *d*), 4.09 (2H, *t*), 3.14 (9H, *s*), 1.08 (2H, *q*), 0.18 (2H, *t*).

The scheme for the molecular composition were shown in the below.

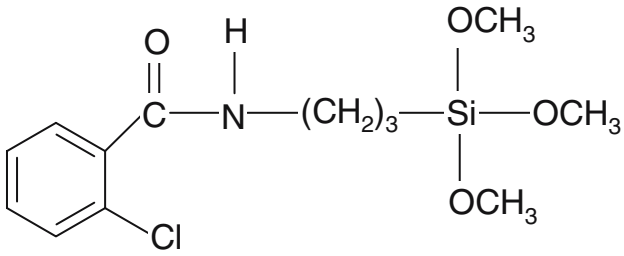

CBA-APMS

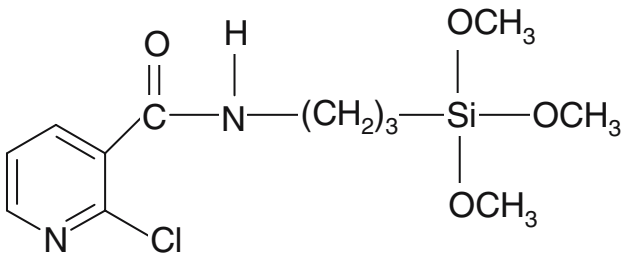

CNA-APMS

Sol–gel polymerization

Sol–gel derived hybrid material containing rare earth was prepared as follows: the synthesized precursor CBA–APMS/CNA–APMS was dissolved in ethanol and tetraethoxysilane (TEOS) and H_2O were added while stirring, and then one drop of diluted hydrochloric acid was added to promote hydrolysis. A stoichiometric amount of RE^{3+} (Tb^{3+} and a different ratio blend of RE^{3+} nitrate) was added to the final stirring mixture. The mole ration of RE^{3+}/CNA–APMS/TEOS/H_2O was 1:3:6:24. After the treatment of hydrolysis, 2 ml dimethylformamide (DMF) and an appropriate amount of hexamethylenetetramine were added to adjust the PH value to about 6.5. The mixture was stirred to achieve a single phase and thermal treatment was performed at 60 ºC until the sample solidified. The hybrid material prepared from Tb^{3+} was denoted as hybrid Tb^{3+}. Using the same method, we also prepared Tb^{3+} and Gd^{3+} co-hybrid materials by mixing Tb^{3+} and Gd^{3+} at different ratios (Tb^{3+}: Gd^{3+}=1:2, 1:1, 2:1) and denoted these as hybrid12, hybrid11, hybrid21, respectively. Schematic illustration of Tb^{3+}–Gd^{3+} cohybrids is seen in Fig. 2.

Characterization

Infrared spectroscopy was obtained in KBr pellets and recorded on a Nexus 912 AO446 FT-IR spectrophotometer in the range of 4,000–400 cm^{-1}. ^{1}HNMR spectra were recorded in DMSO on a Bruker AVANCE-500 spectrometer with tetramethylsilane (TMS) as internal reference. Ultraviolet absorption spectra of these power samples (5×10^{-4} mol/l dimethylformamide (DMF) solution) were recorded with an Agilent 8453 spectrophotometer. Luminescence excitation and emission spectra were obtained on

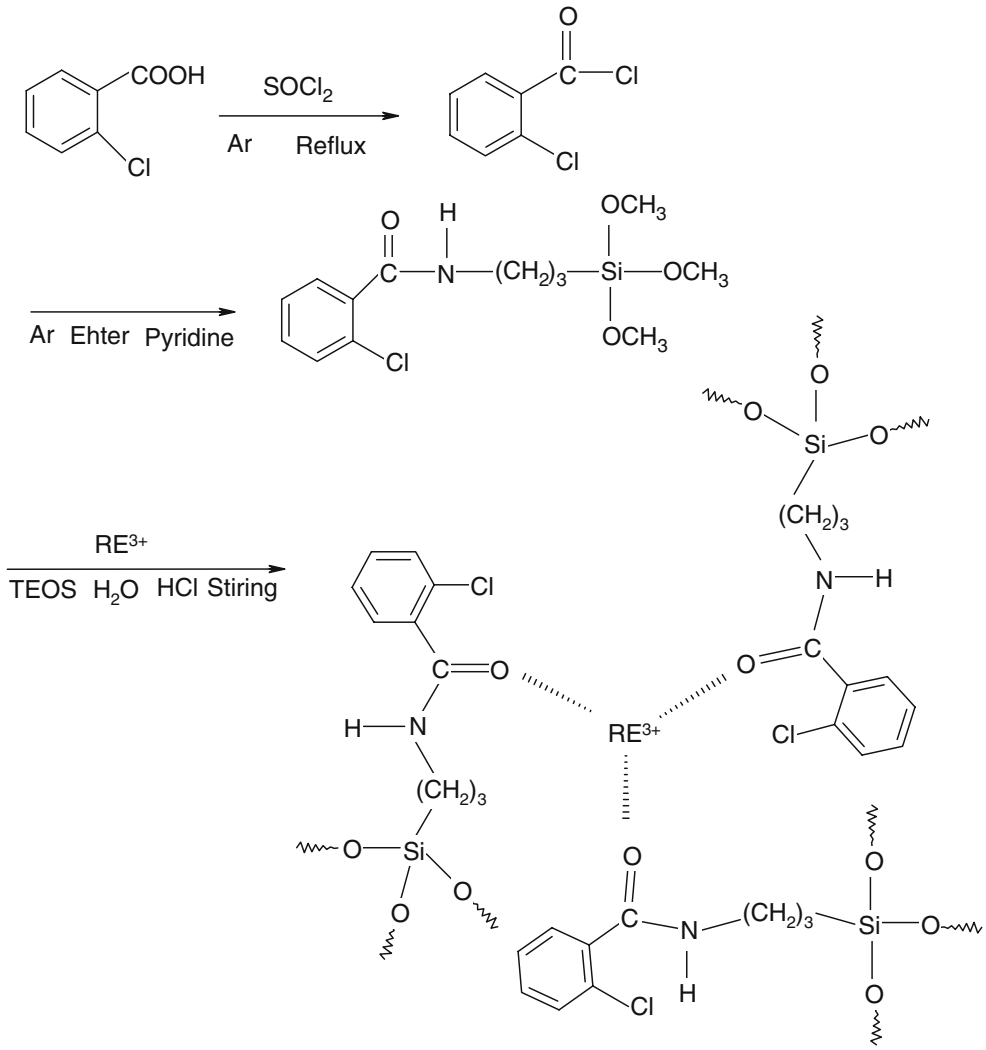

Fig. 1 Scheme of the synthesis process of CBA–APMS ligand and predicted structure of resulting hybrid systems, CBA–APMS shows the similar process

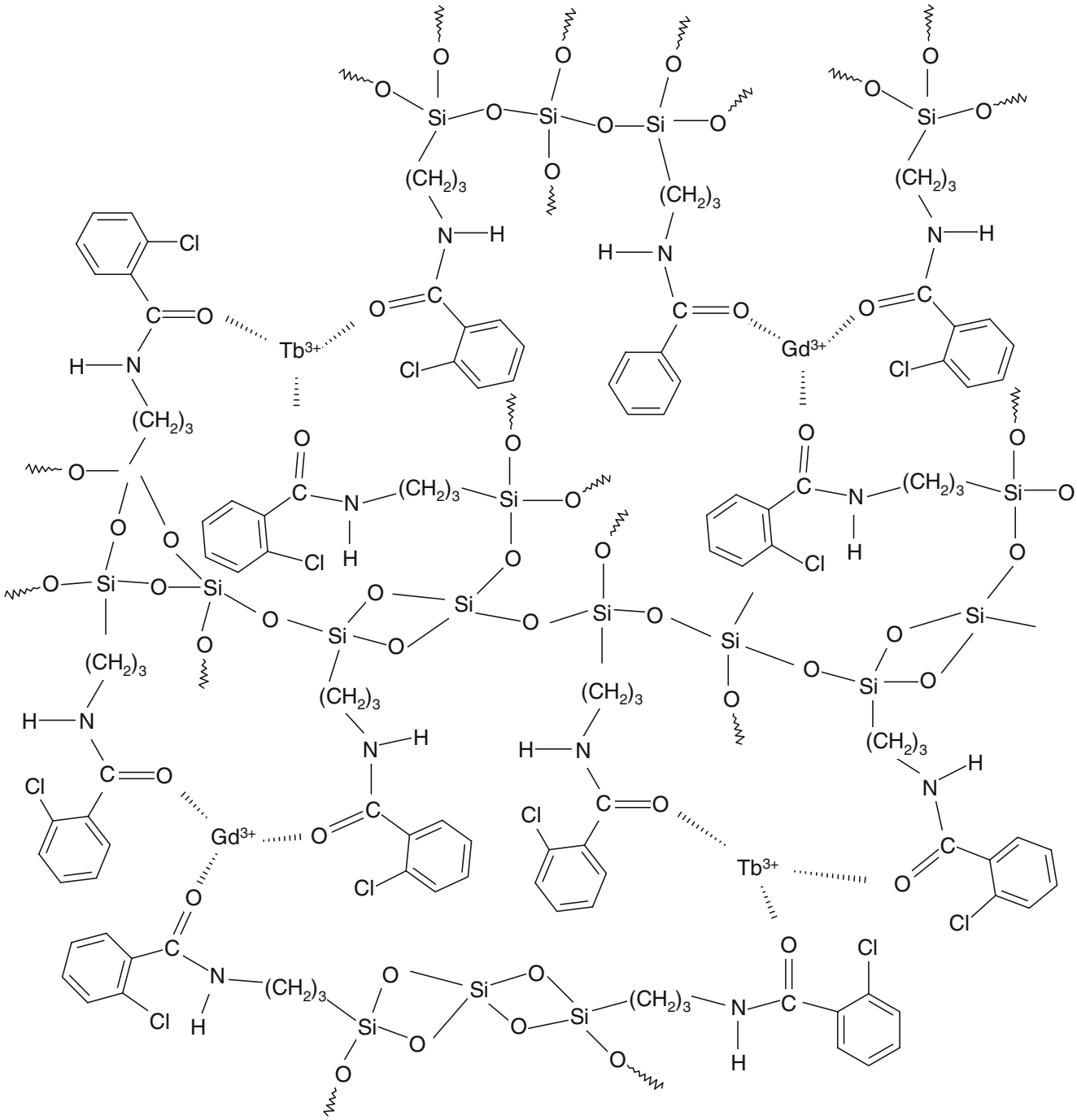

Fig. 2 Schematic illustration of Tb^{3+}–Gd^{3+} co-hybrids

a Perkin–Elmer LS-55 spectrophotometer: excitation slit width=1.5 nm, emission slit width=3.0 nm. All measurements were completed under room temperature.

Results and discussion

The formation of acylamino groups and Si–O–Si network were proved by IR spectroscopy data shown in Fig. 3. As for the CBA–APMS spectra in Fig. 3Ib and CNA–APMS spectra in Fig. 3IIb, the appearance of the bands were located at around 1,640 cm^{-1} due to the absorption of amide groups (CONH) and the presence of the bending vibration (δ_{NH}, 1,540 cm^{-1}), suggesting that 3-amino-propyl-trimethoxysilane has been successfully grafted onto 2-chlorobenzoic acid/2-chloronicotinic acid. Comparing the spectra CBA–APMS (Fig. 3Ib) with the spectra of CBA (Fig. 3Ia) and the spectra of CNA–APMS (Fig. 3IIb) with

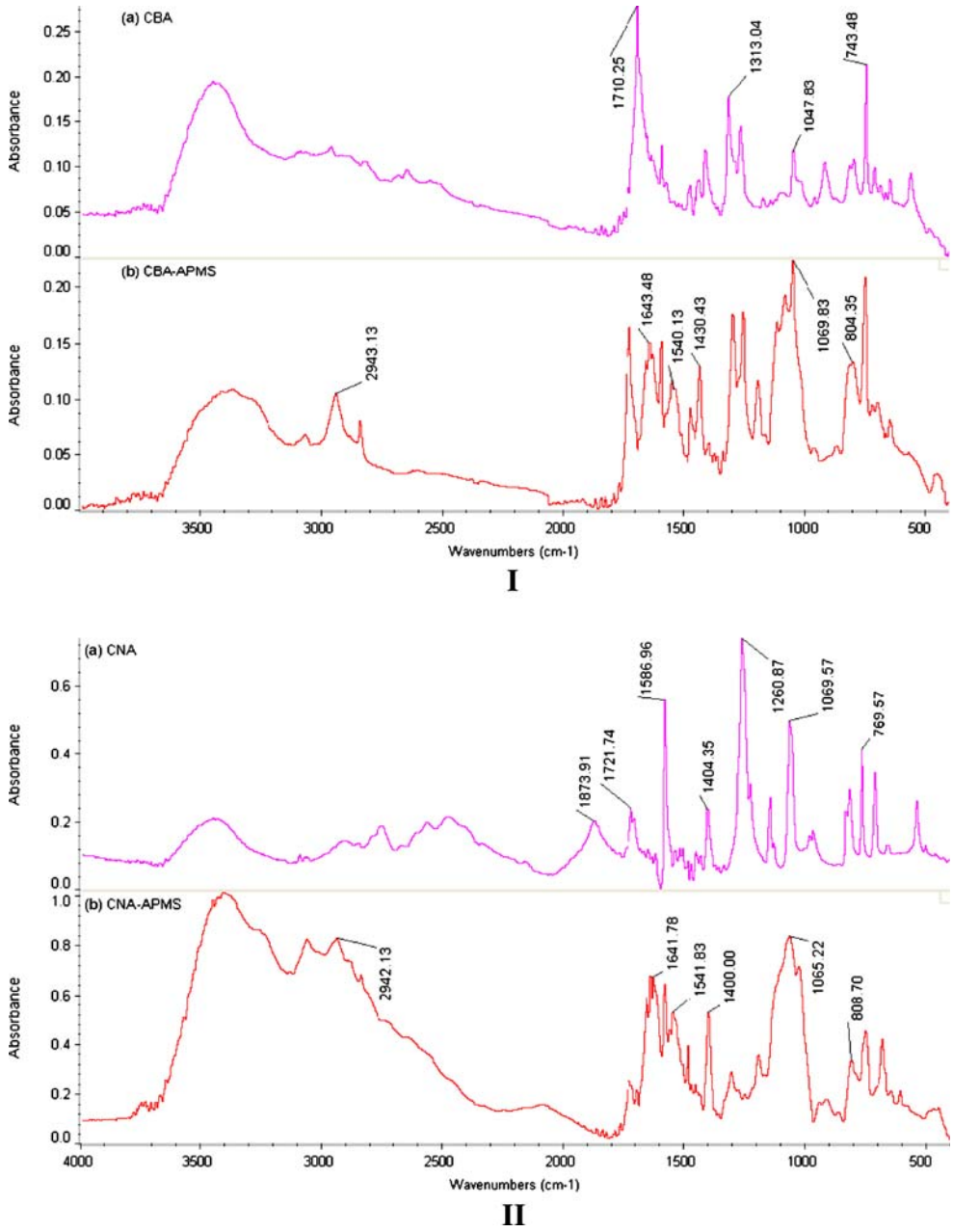

Fig. 3 FT-IR spectra of I**a** CBA, I**b** CBA–APMS and II**a** CNA, II**b** CNA–APMS

the spectra of CNA (Fig. 3IIa), the stretching vibration (υ_{Si-O}) located at around 1,070 cm^{-1} exists, which is evidence of the emergence of CBA–APMS and CNA–APMS.

In addition, the ^{1}HNMR spectroscopy can also explain the structure of CBA–APMS and CNA–APMS. For the ^{1}HNMR spectroscopy of CBA–APMS, the peaks at chemical shifts of about 7.86, 7.45, 7.40 and 7.23 ppm correspond to the H of the aromatic ring. The chemical shift of 8.01 ppm belongs to the H of NH, 3.11 ppm belongs to –O–CH_3– and 0.21 ppm belongs to –CH_2–Si–. For the ^{1}HNMR spectroscopy of CNA–APMS, the peaks at chemical shifts of about 8.41, 8.24 and 7.68 ppm correspond to the H of the heterocyclic ring. The chemical shift of 7.51 ppm belongs to the H of NH, 3.14 ppm belongs to –O–CH_3– and 0.18 ppm belongs to –CH_2–Si–

Figure 4I shows the ultraviolet absorption spectra of (a) CBA, (b) CBA–APMS and (c) hybrid Tb^{3+}, and Fig. 4II shows the ultraviolet absorption spectra of (a) CNA, (b) CNA–APMS and (c) hybrid Tb^{3+}. From the spectra, we find a blue shift of the major $\pi-\pi^*$ electronic transitions (from 274 to 268 nm and from 273 to 269 nm), indicating that modification of 2-chlorobenzoic acid and 2-chloronicotinic acid, which was grafted by 3-aminopropyl-trimethoxysilane, influences its corresponding absorption spectrum. Furthermore, an obvious red shift is observed when we add Tb^{3+} to CBA–APMS (from 268 to 278 nm)

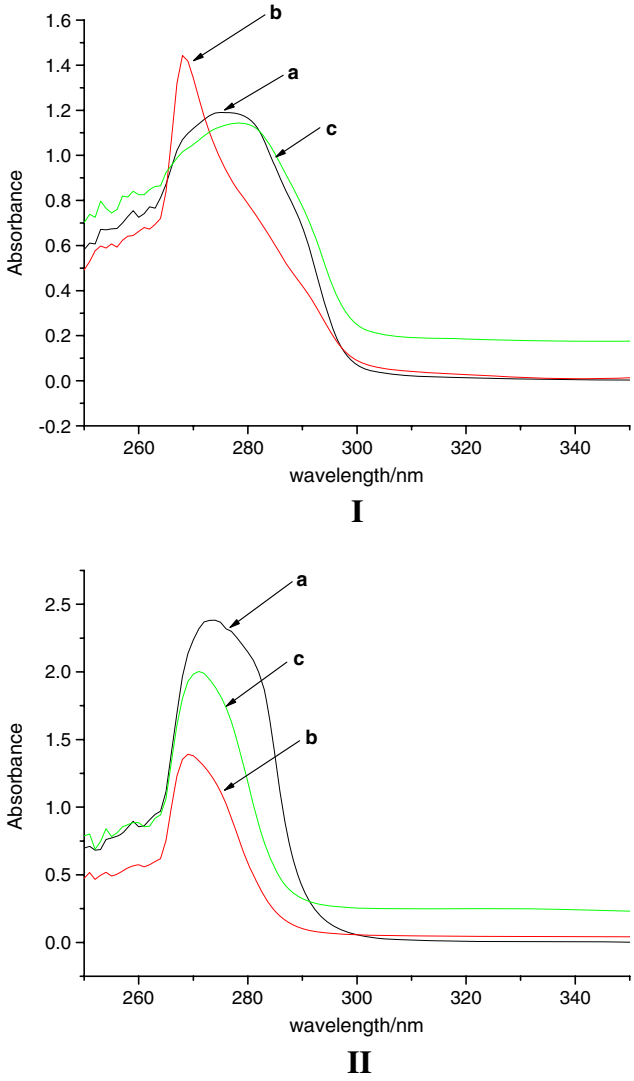

Fig. 4 Ultraviolet absorption spectra for I**a** CBA, I**b** CBA–APMS, I**c** hybrid Tb^{3+} and II**a** CNA, II**b** CNA–APMS, II**c** hybrid Tb^{3+}

and CNA–APMS (from 269 to 272 nm), providing the formation of a complex between Tb^{3+} and CBA–APMS/CNA–APMS.

Figure 5 wears the low-temperature phosphorescence spectra of hybrid 11, hybrid Tb^{3+} for RE^{3+}–CBA–APMS and hybrid 11 and hybrid Tb^{3+} for RE^{3+}–CNA–APMS at 77 K. It can be seen that the phosphorescence intensity of hybrid 11 is strengthened compared with that of hybrid Tb^{3+} while a red shift or blue shift doesn't occur when Gd^{3+} is added. So we can get such a conclusion that the inert ions (such as Gd^{3+}) can strengthen the efficiency of luminescence.

On the basis of the enhancement of luminescent intensities of active lanthanide ions (such as Eu^{3+} or Tb^{3+}) by inert lanthanide ions (i.e. La^{3+}, Ga^{3+}, Lu^{3+},Y^{3+}) in solution systems or solid complexes, we intercalated different ratios of Tb^{3+} and Gd^{3+} into co-hybrid molecular materials through the chemical bonded Si–O network after the co-hydrolysis and co-polycondensation process. The excitation and emission spectra of (a) hybrid 11, (b) hybrid 21, (c) hybrid Tb^{3+}, (d) hybrid 12 for CBA–APMS–RE^{3+} and CNA–APMS–RE^{3+} are shown in Figs. 6 and 7, it can be seen that all the systems have similar excitation spectra that are dominated by a broad band from 280 to 360 nm (for CBA–APMS–RE^{3+}) with the maximum peak at about 326 nm and from 310 to 380 nm (for CNA–APMS–RE^{3+}) with the maximum peak at about 341 nm. The emission lines of hybrid material are assigned to the characteristic $^5D_4-^7F_J$ (J=6, 5, 4, 3) transitions of Tb^{3+} at 488.5, 543, 584 and 616 nm, respectively, and the florescence intensity at 543 nm is the strongest for the $^5D_4-^7F_5$ emission which is the most prominent one. From the excitation spectrum, when Tb^{3+}, Gd^{3+}=1:1 the intensity of the spectrum was stronger than others. Corresponding to the excitation

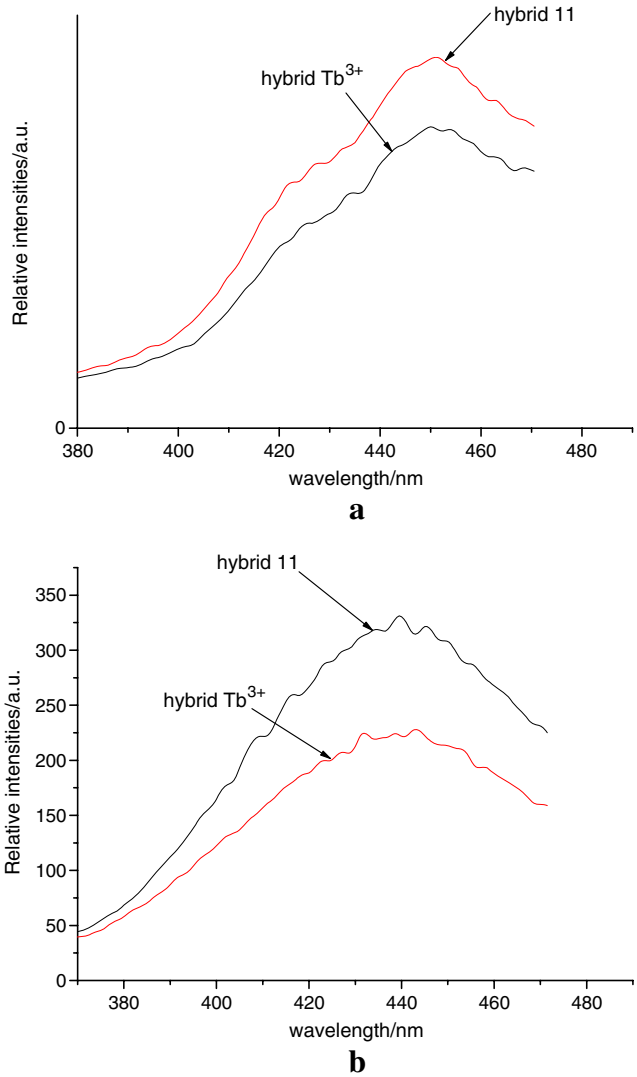

Fig. 5 The phosphorescent spectra of **a** hybrid 11 and hybrid Tb^{3+} for RE^{3+}–CBA–APMS, **b** hybrid 11 and hybrid Tb^{3+} for RE^{3+}–CNA–APMS

spectrum, the fluorescent intensities of hybrids changed with the same sequence.

Although CBA/CNA can sensitize Tb^{3+} and hybrid Tb^{3+} can exhibits good luminescence characteristics, its intensity is not strong. But when Gd^{3+} is added to the hybrid Tb^{3+}, the luminescence intensity of hybrids is much enhanced; and this is a newly found co-luminescence system. Extensive emission intensity and narrow half emission width (below 15 nm) were observed, which show the luminescence characteristics of the resulting hybrid materials.

From Figs. 6 and 7, it can be seen that the luminescence intensity of the hybrids was weakened along with the reduction of the active luminescent center (Tb^{3+}) which was brought by the enhancement of inert ions' (Gd^{3+}) concentration. So we can make such a conclusion: when Gd^{3+} and Tb^{3+} are added to molecular hybrid material at an appropriate ratio, the intrinsic emission peaks of Tb^{3+} are much enhanced. The mechanism of this co-luminescence enhancing effect is as follows. It is proverbial that CBA and CNA can absorb radiant energy and then transfer it to Tb^{3+}. Because the rare earth nitrates hydrolyze and polymerize together with CBA–APMS/CNA–APMS and TEOS, we consider that Tb^{3+} and Gd^{3+} exist in the same molecular hybrids at molecular degree through the chemical bonded Si–O network. It can be presumed that the intramolecular energy transfer occurs and the transfer process from the energy donor (CBA–APMS/CNA–APMS) to Tb^{3+} is enhanced, which agrees with the similar phenomenon in other systems [26]. In this sort of co-luminescence system, the distance between Tb–CBA–APMS/Tb–CNA–APMS and Gd–CBA–APMS/Gd–CNA–APMS is very small, the energy of CBA–APMS/CNA–APMS in the Gd–CBA–APMS/Gd–CNA–APMS can be transferred to Tb^{3+} through intramolecular energy transfer, which lead to the enhanced luminescence of Tb^{3+} in the hybrids. From Fig. 2, we can see that each of Tb–CBA–APMS/Tb–CNA–APMS molecular fragments is surrounded by many Gd–CBA–APMS/Gd–CNA–APMS molecular fragments, then these

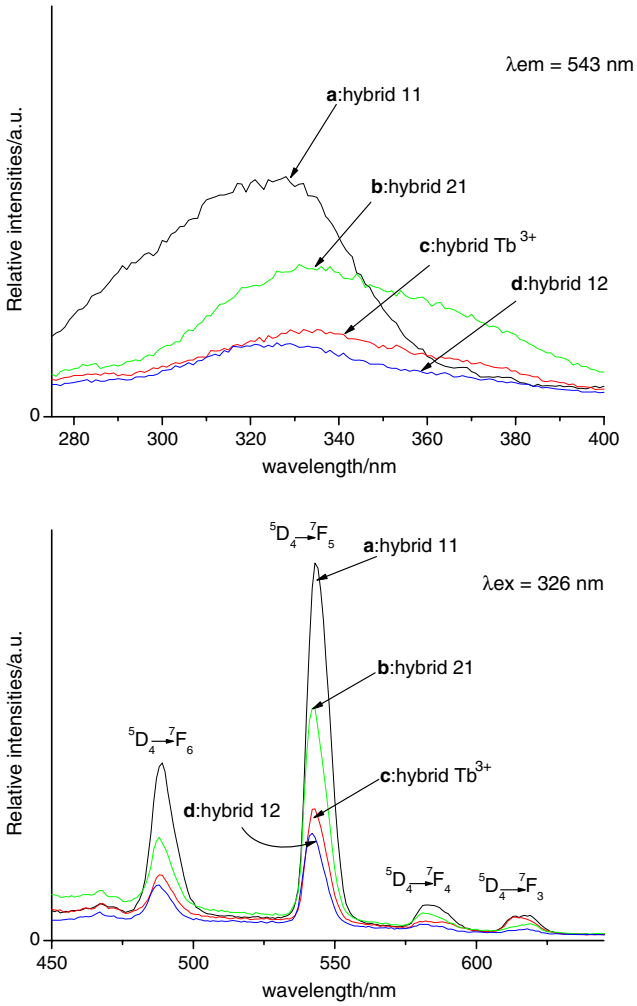

Fig. 6 Excitation spectrum and emission spectra of **a** hybrid 11, **b** hybrid 21, **c** hybrid Tb^{3+} and **d** hybrid 12 for RE^{3+}–CBA–APMS

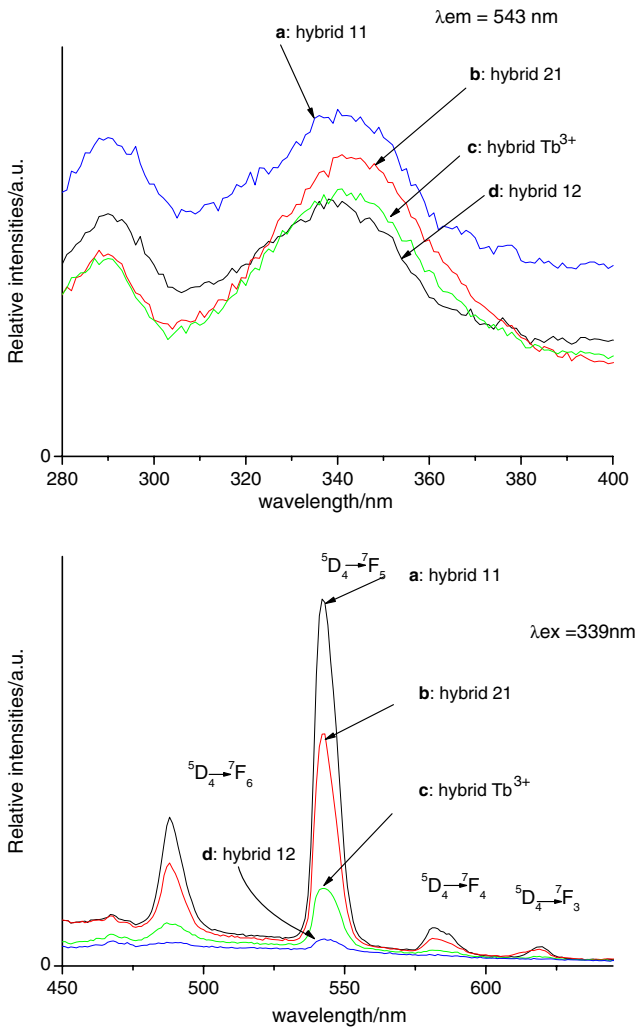

Fig. 7 Excitation spectrum and emission spectra of **a** hybrid 11, **b** hybrid 21, **c** hybrid Tb^{3+} and **d** hybrid 12 for RE^{3+}–CNA–APMS

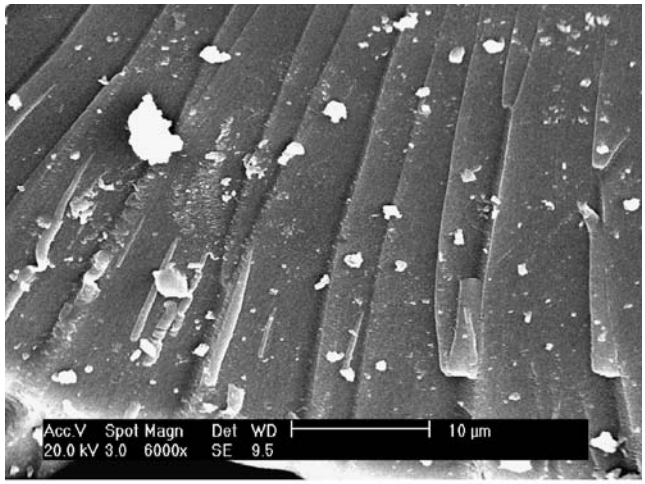

a

b

Fig. 8 SEM diagraphs of **a** Tb^{3+}–CBA–APMS and **b** Tb^{3+}–CNA–APMS molecular-based hybrids

Gd–CBA–APMS/Gd–CNA–APMS molecular fragments form a cage which acts as an energy-insulating sheath that can prevent collision with water molecules and decrease the energy loss of Tb–CBA–APMS/Tb–CNA–APMS, thus luminescence quantum efficiency and luminescence intensity have been improved greatly.

In addition, from Figs. 6 and 7, the characteristic emission of Gd^{3+} is not observed. This is due to the fact that Gd^{3+} possesses a relatively stable half-filled 4f shell and the excited state of Gd^{3+} is higher than the triplet start of CBA–APMS/CNA–APMS, so the energy of CBA–APMS/CNA–APMS cannot be transferred to Gd^{3+} by an intramolecular energy transfer process.

From Fig. 8a, we can see that the scanning electron micrograph looks like the trunk of pine trees, which demonstrates that rare earth complexes were dispersed within silica homogenously due to covalent bonds bridged between different phases. So we can conclude that the hybrid Tb^{3+} is apt to grow into infinite chainlike structure from the microstructure view and retain the coordinated positions in corresponding bulk materials. In the process of co-hydrolysis and polycondensation, the structure of hybrids can be formed according to different kinds of competitive mechanism. The first one is the tendency to form the one-dimensional chainlike structure which due to the ligand composed of 2-chlorobenzoic acid, and the second one is the tendency to form the polymeric network structure of Si–O, but the first one plays a primary role. So in this way, the trunk structure was achieved for the dominant growth along the terbium coordination polymer chain in the former, while the latter formed normally homogeneous materials. The scanning electron micrograph of Fig. 8b demonstrates that a homogeneous, molecular-based material was obtained where no phase separation was observed because of strong covalent bonds bridging between the inorganic and organic phases.

Conclusion

In summary, we have modified 2-chlorobenzoic acid and 2-chloronicotinic acid successfully with a cross-linking molecule 3-aminopropyl-trimethoxysilane, and gained a functional bridge molecule. Then through the in-situ sol–gel process (cohydrolysis and copolycondensation process) of the alkyl groups, terbium and gadolinium ions can be assembled in the same molecular hybrid systems though the chemical bond. On the one hand, it can coordinate to rare earth ions through carbonyl groups; on the other hand, the hydrolysis and polycondensation reactions between triethoxysilyl of CBA–APMS/CNA–APMS and TEOS lead to the formation of Si–O–Si network structures for the same alkoxy groups of them. A series of luminescent molecular-based hybrid materials were firstly constructed using CBA–APMS/CNA–APMS coordinated to Tb^{3+} and.Gd^{3+}. As Tb^{3+} and Gd^{3+} exist in the same molecule, the fluorescent enhancement effect occurs and is discussed in this paper. This technology can be expected in the assembly of other luminescent molecular-based hybrid material.

Acknowledgement This work was supported by the National Natural Science Foundation of China (20671072).

References

1. Suratwala T, Gardlund Z, Davidson K, Uhlmann DR (1998) Silylated coumarin dyes in sol–gel hosts. II. Photostability and sol–gel processing. Chem Mater 10:190

2. Molina C, Dahmouche K, Santilli CV (2001) Structure and luminescence of Eu3+-doped class I siloxane-poly(ethylene glycol) hybrids. Chem Mater 13:2818
3. Matthews LR, Knobbe ET (1993) Luminescence behavior of europium complexes in sol–gel derived host materials [J]. Chem Mater 5:1697
4. Casalboni M, Senesi R, Prospositio P (1997) Rigid-cage effects on the optical properties of the dye 3,3′-diethyloxadicarbocyanine incorporated in silica–gel glasses. Appl Phys Lett 30:2969
5. Lebeau B, Fowler CE, Hall SR (1999) Transparent thin films and monoliths prepared from dye-functionalized ordered silica mesostructures. J Mater Chem 9:2279
6. Innocenzi P, Kozuka H, Yoko TJ (1997) Luminescence properties of the. $Ru(bpy)_3^{2+}$ complex incorporated in sol-gel-derived silica coating. Films J Phys Chem B 101:2285
7. Mstsui K, Momose F (1997) Luminescence properties of tris(2,2′-bipyridine)ruthenium(II) in sol–gel systems of SiO_2. Chem Mater 9:2588
8. Harreld JH, Esaki A, Stucky GD (2003) Low-shrinkage, high-hardness, and transparent hybrid coatings: poly(methyl methacrylate) crosslinked with silsesquioxane. Chem Mater 15:3481
9. Minoofar PN, Hernandez R, Chia S, Dunn B, Zink JI, Franville AC (2002) Placement and characterization of pairs of luminescent molecules in spatially separated regions of nanostructured thin films. J Am Chem Soc 124:14388
10. Choi J, Tamaki R, Kim SG, Laine RM (2003) Organic/inorganic imide nanocomposites from aminophenylsilsesquioxanes. Chem Mater 15:3365
11. Franville AC, Zambon D, Mahiou R, Chou S, Troin Y, Cousseins JC (1998) Synthesis and optical features of europium organic–inorganic silicate hybrid. J Alloys Compd 275–277:831
12. Li HR, Fu LS, Zhang HJ (2002) Luminescence properties of transparent hybrid thin film covalently linked with lanthanide complexes. Thin Solid Films 416:197
13. Li HR, Lin J, Zhang HJ, Fu LS (2001) Novel, covalently bonded hybrid materials of europium (terbium) complexes with silica [J]. Chem Commun 1212
14. Dong DW, Jiang SC, Men YF, Ji XL, Jiang BZ (2000) Nano-structured hybrid organic–inorganic lanthanide complex films produced in situ via a sol–gel approach. Adv Mater 12:646
15. Liu FY, Fu LS, Zhang HJ (2003) Luminescent film with terbium-complex-bridged polysilsesquioxanes. New J Chem 27:233
16. Franville AC, Zambon D, Mahiou R (2000) Luminescence behavior of sol–gel-derived hybrid materials resulting from covalent grafting of a chromophore unit to different organically modified alkoxysilanes. Chem Mater 12:428
17. Li HR, Lin J, Fu LS, Guo JF, Meng QG, Liu FY, Zhang HJ (2002) Microporous Mesoporous Mater 55:103
18. Hobson ST, Shea KJ (1997) Bridged Bisimide polysilsesquioxane xerogels: new hybrid organic–inorganic materials. Chem Mater 9:616
19. Wang QM, Yan B (2004) Novel luminescent terbium molecular-based hybrids with modified meta-aminobenzoic acid covalently bonded with silica. J Mater Chem 14:2450
20. Nandi M, Conklin JA, Salvati L, Sen A (1990) Molecular level ceramic/polymer composites 1. Synthesis of polymer-trapped oxide nanoclusters of chromium and iron. Chem Mater 2:772
21. Liu FY, Fu LS, Zhang HJ (2003) Luminescent film with terbium-complex-bridged polysilsesquioxanes. New J Chem 27:233
22. Li HR, Fu LS, Zhang HJ (2002) Luminescence properties of transparent hybrid thin film covalently linked with lanthanide complexes. Thin Solid Films 416:197
23. Choi J, Tamaki R, Kim SG, Laine RM (2003). Organic/inorganic imide nanocomposites from aminophenylsilsesquioxanes. Chem Mater 15:3365
24. Wang QM, Yan B (2004) Novel luminescent molecular-based hybrid organic–inorganic terbium complex covalently bonded materials via sol–gel process. Inorg Chem Commun 7:747
25. Yang JH et al (1989) Application of the columinescence effect of rare earth: simulataneous determination of trace amounts of samarium and europium in solution. The Analyst 114:1417
26. Xu YY, Hemmila I (1992) Co-fluoresence enhancement system based on pivaloyltrifluoroacetone and yttrium for the simultaneous detection of europium, terbium, samarium and dysprosium. Anal Chim Acta 9:256
27. Sato S, Wada M (1970) Relations between intramolecular energy transfer efficiencies and triplet state energies in rare earth 3-diketone chelates [J]. Bull Chem. Soc Jpn 43:1955